



## **A parametric study on the mesostructure design and stiffness of tow-based discontinuous composites using a voxel finite element model**

Downloaded from: <https://research.chalmers.se>, 2025-10-15 01:36 UTC

Citation for the original published paper (version of record):

Gulfo Hernandez, L., Katsivalis, I., Asp, L. et al (2025). A parametric study on the mesostructure design and stiffness of tow-based discontinuous composites using a voxel finite element model. *Composites Science and Technology*, 272. <http://dx.doi.org/10.1016/j.compscitech.2025.111369>

N.B. When citing this work, cite the original published paper.



# A parametric study on the mesostructure design and stiffness of tow-based discontinuous composites using a voxel finite element model

Luis Gulfo<sup>a,b</sup>, Ioannis Katsivalis<sup>a,b,c</sup>, Leif E. Asp<sup>a,b</sup>, Martin Fagerström<sup>a,b</sup>

<sup>a</sup> Department of Industrial and Materials Science, Chalmers University of Technology, Sweden

<sup>b</sup> TechForH2 Competence Centre, Chalmers University of Technology, Sweden

<sup>c</sup> Department of Architecture and Civil Engineering, University of Bath, UK

## ARTICLE INFO

### Keywords:

Discontinuous reinforcement  
Tow-based composites  
Parametric study  
Mechanical properties  
Finite element analysis  
Mesostructural effects  
Elastic behaviour

## ABSTRACT

Tow-Based Discontinuous Composites (TBDCs) are manufactured by compression moulding of randomly deposited carbon fibre tows. As such, a quasi-isotropic response with high stiffness and strength can be achieved, while reducing waste, thus competing with laminated composites. Moreover, novel TBDCs with ultra-thin tows (0.02 mm) have expanded the design space and opened opportunities for thin-walled structures. However, complex 3D mesostructural parameters have been demonstrated to impact their stiffness, such as tow/plate morphology, resin pocket content, tow waviness, and tow orientation distributions, which remain a challenge for their modelling and design. The present work exploits a novel voxel-based finite element mesostructure generator for TBDCs developed and validated by the authors to explore the significance of mesostructural design modifications on their stiffness. A parametric study over an extended design space including baselines of thick, thin, and ultra-thin tow systems, is conducted to investigate the effect of important parameters such as the tow moduli (up to ultra-high modulus), tow and plate dimensions (with attention to thin plates), and preferred in-plane fibre orientation distributions. Also, the significance of the numerical model is compared with short-fibre models and equivalent laminates. The results compare their sensitivity for each TBDC material system, showing opportunities for optimisation. Finally, design constraints are identified in terms of the stiffness knockdown, quasi-isotropic behaviour, statistical variability of the elastic properties, and critical minimum plate dimensions.

## 1. Introduction

Over the last decade, there has been an increasing use of discontinuous composites in aviation. In particular, Tow-Based Discontinuous Composites (TBDCs), manufactured using compression moulding with randomly deposited prepreg tows, have replaced metals to reduce weight of e.g. window frames and airframe brackets [1]. Recent studies have demonstrated the potential use of TBDCs in demanding applications, due to their high performance in terms of quasi-isotropic stiffness and tensile strength [2,3], fatigue resistance [4], and hydrogen permeability [5], while being lighter than aircraft grade aluminium. Moreover, the scrap material is minimised, the manufacturability is enhanced, and thus the design space is expanding.

While TBDCs offer the previous advantages, the characterisation and certification of the stiffness and strength of discontinuous composites for aircraft remain a challenge, as they currently rely on costly experimental campaigns because of their random 3D microstructure and variable mechanical properties [6,7]. Although this approach leads

to suboptimal/overweighted designs [8], limited efforts have been made to certify TBDCs via numerical analysis [6]. Also, attention has been restricted to prototype materials, like HexMC<sup>®</sup> M77 by Hexcel [9] with a standard aircraft tow thickness (0.127 mm). Recently, new TBDCs have been developed with ultra-thin spread tows (TeXtreme<sup>®</sup> 360° by Oxeon AB [10]), considerably expanding the design space. Thus, there is a lack of numerical studies exploring the new design space of different TBDCs, that provide methods for analysing their mesostructural design and stiffness.

The extensive design space arises from the various parameters involved during manufacturing (Fig. 1(a)), which involves three stages [9]: (1) a chopper is used to cut a unidirectional (UD) prepreg of thickness  $t$ , into tows with length  $l$ , and width  $w$ ; (2) an uncured plate is assembled by placing the tows with a random in-plane fibre orientation distribution (FOD)  $\theta$ ; (3) the plate is cured to a thickness  $t_p$  by compression moulding. During moulding, material flow can be induced,

\* Corresponding author at: Department of Industrial and Materials Science, Chalmers University of Technology, Sweden.  
E-mail address: [gulfo@chalmers.se](mailto:gulfo@chalmers.se) (L. Gulfo).

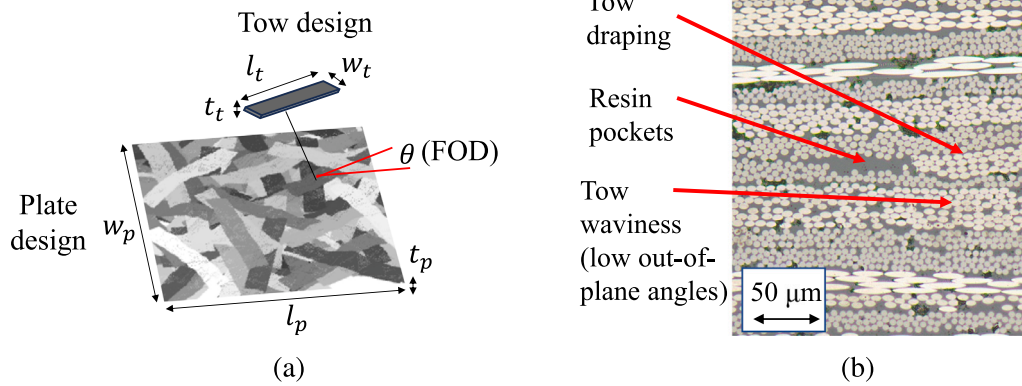


**Fig. 1.** Morphology of TBDCs. (a) Nominal tow and plate design parameters on a virtual specimen, (b) Cross-section of an ultra-thin tow TBDC showing typical microstructural features.

allowing to generate plates with a preferred in-plane FOD (“high-flow” case) or a random FOD (“low-flow” case) [11]. In-mould flow during manufacturing has been shown to have a strong effect on the microstructure and mechanical properties of moulding compounds [12, 13], resulting in a different response compared to perfectly aligned prepreg tow composites [14]. Additionally, from tow thicknesses found in the literature and manufacturers data, this work proposes a broad classification, where TBDCs are classified as thick ( $\approx 0.3$  mm), thin ( $\approx 0.15$  mm), and ultra-thin ( $\approx 0.02$  mm), highlighting the numerous design options.

The resulting 3D microstructure of TBDCs is highly dependent on the tow design and compression moulding. As shown in Fig. 1(b), tow interactions during compaction generate 3D local variations of the tow waviness (out-of-plane angles), tow draping (i.e. wrapping over tow ends), tow shape, resin pockets, voids, and volume fraction (VF) of fibres. Li et al. [15] showed that such features are affected by the tow thickness, where TBDCs with thicker tows present a geometrical variability with significant out-of-plane orientations. In contrast, TBDCs with thinner tows display a more “layered” structure (Fig. 1(b)).

Several studies have assessed the effect of different material and morphology parameters on the mechanical response of TBDC plates, as presented in Table 1. Feraboli et al. [16] experimentally characterised a carbon fibre/epoxy TBDC by testing in tension, compression, and bending. Tow lengths between 12.7–76.2 mm were tested, with a fixed tow thickness of 0.127 mm and a width of 8.4 mm or 4.1 mm. Plate thicknesses of 2, 3 and 6 mm were tested. A slightly increasing trend of the tensile modulus with respect to the tow length was reported, while a strong dependence was found between the tensile modulus and the plate thickness. However, only three specimens were tested per configuration, and property variations were in the range of 8% to 43%, suggesting the need for more extensive testing. Selezneva and Lessard [17] tested a carbon fibre/PEEK TBDC under tension, compression, shear, and fatigue for different in-plane tow sizes. For each case, eight specimens were tested with a fixed tow thickness of 0.14 mm and a plate thickness of 2.5 or 6 mm. It is highlighted that plates were produced by shuffling the tows, affecting the achieved randomness and variability. Increasing trends were reported for the tensile modulus with respect to the tow size, but no significant effect of plate thickness was found in this case. It was difficult to see any trends given the high variability in the properties.

As an alternative to costly experiments, few numerical studies have investigated the parametric design of TBDCs for stiffness response. Alves and Pimenta [18] developed a 3D mesostructure generator combined with an analytical stiffness model, which demonstrated the significant influence of tow waviness on the stiffness (up to 25% reduction). They show as well the limitation of 2D models without waviness due to overpredictions in the tensile properties. Additionally, a parametric analysis was presented, addressing independently the effect of the tow

dimensions and the plate thickness, within the ranges in Table 1. For this, the baseline was restricted to a carbon fibre/epoxy TBDC with a nominal tow thickness of 0.164 mm (HexMC® M77). Also, one case with preferred FOD was studied. It should be noted that the tow VF was assumed to be 100% (i.e. 0% of resin pockets). Kravchenko et al. [19] studied the effect of the tow thickness (0.05–0.25 mm), the plate thickness (0.8–7 mm), and in-plane FOD (low-flow and high-flow) on stiffness. Both lower tow thicknesses and more aligned FODs improved the stiffness. However, once more the resin pocket content was neglected.

Ko et al. [20] investigated the effect of the resin pocket VF between 4 and 8% for a material having a tow thickness of approximately 0.14 mm and a high length-to-width aspect ratio (AR). The reduction in resin pocket VF for the given range led to an increase of up to 7% in the tensile modulus, although the predicted trend was not investigated down to ultra-thin tows. Since the resin pocket content and FODs depend on the tow size [17], and the tow VF is linked to the compaction state during the compression moulding (increasing from around 30% after deposition to 97% in the cured plate) [23], the combined effect with resin pockets on the stiffness requires further study.

Capturing 3D mesostructural features in numerical models, like resin pockets and waviness, is key for the parametric analysis of TBDCs. A review of different modelling approaches can be found in the authors’ recent publication [24]. Therein, the authors developed and validated a novel 3D voxel mesostructure generator based on a Random Sequential Absorption (RSA) technique that combines a bin-guided tow deposition, a tow draping algorithm, and a strategy to control plate thickness variations. These reproduce the resin pocket content, tow waviness, and in-plane and out-of-plane angle distributions within values reported in the literature. The numerical framework uses 3D computational homogenisation and its ability to accurately predict elastic properties was validated for thick, thin, and ultra-thin tow TBDCs. A parametric study exploiting the capabilities of such a framework for different TBDC systems is currently lacking in the literature.

Given the emerging TBDC material systems and technology, there is a lack of research on their extended design space and mechanical behaviour, including ultra-thin tow cases, necessary to assess lighter, thinner, and high-stiffness driven designs. In this context, the previous studies (Table 1) have the following limitations. Experimental studies are limited by the cost of producing several specimens to account for variability and ensure statistically representative testing while adjusting the parameters. A tow thickness between 0.12 and 0.14 mm is used as a baseline for most analyses. In certain cases a value down to 0.05 mm has been explored. This does not cover ultra-thin tows as low as 0.021 mm. In turn, relatively large plate thicknesses have been investigated, hence critical constraints for ultra-thin cases are uncertain. In addition, a resin pocket VF of 0% is typically assumed

**Table 1**

Tow and TBDC plate parameters studied in the literature.

Parameters			Study [16] Exp.	[17] Exp.	[18] Numer.	[19] Numer.	[20] Numer.
Tow	Material		Carbon epoxy	Carbon PEEK	Carbon epoxy	Carbon PEKK	Carbon PEKK
	Thickness $t_t$	mm	0.127	0.14	0.05–0.2	0.05–0.25	0.14
	Length $l_t$	mm	12.7–76.2	6–50	10–60 <sup>c</sup>	12.7–50.8 <sup>e</sup>	12.7
	Width $w_t$	mm	4.1, 8.4	3–12	5–30 <sup>c</sup>	12.7	1.6 <sup>f</sup> –12.7
	AR ( $l_t/w_t$ )		1.5–12.5	2–8.3	1.25–10	1–3.94	1 <sup>f</sup> –7.9
	$E_1$	GPa	128 <sup>a</sup>	N/A <sup>b</sup>	131 <sup>d</sup>	130.7	130.7
Plate	$E_2$	GPa	9 <sup>a</sup>	N/A <sup>b</sup>	9 <sup>d</sup>	9.6	9.6
	Thickness $t_p$	mm	2, 4, 6	2.5, 6	1–3 <sup>c</sup>	0.8–7 <sup>e</sup>	1.65–12.7
	Fibre VF $V_f^p$	%	–	–	57.85	–	–
	Resin pocket VF $V_r^p$	%	–	–	0	0	4–7.5
	Laying process		Shuffling	Shuffling	RSA	RSA	RSA
	In-plane FOD		Random	Random	Random, preferred orientation	Random, two preferred orientations	Random

<sup>a</sup> From TORAYCA T700/2510 UD prepreg datasheet [21].<sup>b</sup> Undisclosed due to proprietary information.<sup>c</sup> For a fixed tow thickness baseline (HexMC-M77), with a nominal value of 0.164 mm [22].<sup>d</sup> Scaled from values of tensile tests on HexPly-M77 [22].<sup>e</sup> For a fixed tow thickness baseline (AS4/PEKK), with nominal value of 0.14 mm.<sup>f</sup> Estimated from data. Exact dimension undisclosed due to intellectual property.

in numerical models, a parameter proven to be key for stiffness prediction, and which is related to the tow thickness. Moreover, other values of the resin pocket VF over 4% are not applicable for ultra-thin tow cases. Thus, assessing stiffness variations due to different thicknesses without realistic resin pocket VF overlooks relevant physical constraints (combined effects) and leads to overestimation. Finally, (ultra-) high modulus tows with values larger than 131 GPa have not been investigated in parametric studies.

The present work aims to contribute to the state of the art of TBDCs by exploiting a validated 3D voxel-based FE model to conduct the following parametric numerical study on the stiffness response of TBDCs: (1) explore an extended design space of TBDCs by considering three baselines, covering thick, thin, and ultra-thin tow systems; (2) investigate critically low plate thicknesses and their effect in terms of random tow distributions, quasi-isotropic response, and in-plane sizing of plates; (3) incorporate the effect of realistic resin pocket VF in the stiffness predictions, in accordance with each baseline; (4) in addition to tensile modulus, evaluate the shear modulus for different cases; (5) assess the effect of ultra high-modulus tows; (6) study the out-of-plane angle distributions in relation to the tow design; and (7) consider in-plane tow angle distributions (“high-flow” condition). These contributions open opportunities in material design and stiffness optimisation of TBDCs for light, thin-walled structures.

## 2. Materials and methods

### 2.1. Specification of the material design

The geometrical design of a representative TBDC plate is illustrated in Fig. 1(a). At the tow level, the design is characterised by the nominal dimensions  $l_t \times w_t \times t_t$ , which are the length, width, and thickness, respectively. In order to manufacture the TBDC plate, tows are deposited according to an in-plane (random) orientation distribution  $\theta$ . Then, compression moulding is used to consolidate the final plate design with nominal dimensions  $l_p \times w_p \times t_p$  (length, width, and thickness). The compaction level produces a mesostructure with a specific fibre VF ( $V_f^p$ ), resin pockets VF ( $V_r^p$ ), and in-plane and out-of-plane FODs ( $\varphi$ ), which characterise the morphology of the plate design. This mesostructural design is largely driven by the tow thickness [15], motivating the need for analysing different case studies, addressing thick, thin, and ultra-thin tow TBDCs. In addition, the mechanical properties of tows and resin are specified, as indicated hereafter.

**Table 2**

Baseline of the material properties of the tows and matrix (resin pockets), based on [24]. The properties are used as inputs in the FE model of TBDCs.

Material	Model	Properties
Tow (unidirectional)	Transverse isotropic elastic	$E_1 = 131$ GPa $E_2 = E_3 = 9$ GPa $G_{12} = G_{13} = 5.6$ GPa $G_{23} = 3.2$ GPa $\nu_{12} = \nu_{13} = 0.34$ $\nu_{23} = 0.4$
Matrix (resin pockets)	Isotropic elastic	$E_m = 3.5$ GPa, $G_m = 1.3$ GPa, $\nu_m = 0.35$

### 2.2. Design of the simulation campaign for the parametric study

This section describes the selected design parameters, the proposed simulation campaign, and the baselines for the parametric studies of the different TBDC systems. The proposed modelling methodology experimentally validated in [24] is incorporated in the parametric study as presented in Fig. 2, which is explained in the following.

#### 2.2.1. Model input parameters

As described in Section 2.1, the input tow design is specified by the nominal dimensions  $l_t \times w_t \times t_t$ , as well as its mechanical properties (Table 2). At the plate level, the mean plate thickness  $t_p$  is the key geometrical parameter, and the in-plane size is chosen according to the analysis. Since resin pockets are incorporated in the model, both the VF of resin pockets and the mechanical properties of the resin phase (isotropic) need to be specified. Finally, another input related to the plate design is the FOD corresponding to the (final) in-plane tow angles. In most cases, this consists of a random distribution, except when a preferred in-plane FOD is used, which depends on the manufacturing process. In the present study, a random in-plane FOD is assumed unless explicitly mentioned.

#### 2.2.2. Parametric 3D TBDC mesostructure generator and computational homogenisation

A detailed description of the modelling approach can be found in [24]. This refers to modelling techniques used for TBDC materials, in this context to obtain a voxelised 3D model for finite element analysis. The proposed approach includes the generation of mesostructures (tow voxelisation algorithm, 3D RSA technique, and deposition strategies), the sampling of statistical volume elements, the computational homogenisation, and finally statistical and sensitivity analyses. Important aspects of the modelling are described next:



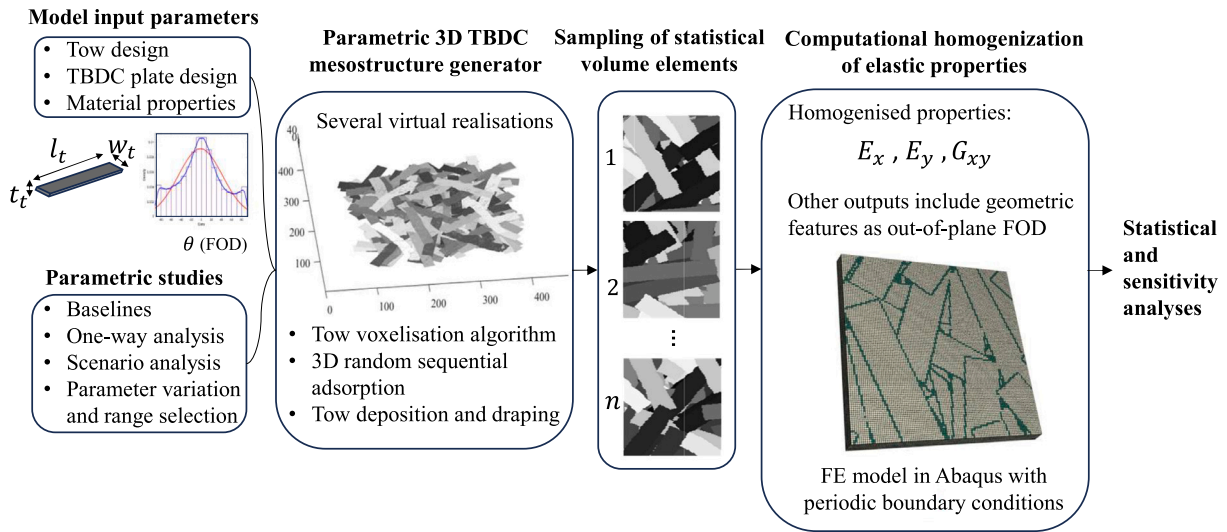


Fig. 2. Proposed methodology for the parametric study, incorporating the parametric 3D TBDC mesostructure generator from [24].

- **Parametric 3D TBDC mesostructure generator:** a voxelisation algorithm is used to voxelise the tows through their length, width and thickness. For the purpose of maintaining an appropriate resolution (linked to the FE mesh), the voxelisation is performed as a function of the thickness, i.e. based on the number of voxels per thickness and the aspect ratios of the voxel across the length and width of the tow. To reduce the computational cost, one voxel through the thickness ( $N_{t,vox,h} = 1$ ) is employed. Since the resulting in-plane voxel aspect ratio  $R_{vox}$  is related to the size of the resin pockets, it requires a suitable choice based on realistic resin pocket VFs. The tow thickness and resin pocket VF have been shown to characterise the processed state of TBDCs, both depending on the heat and pressure applied during the manufacturing [23]. To account for this in the modelling, realistic values for the consolidated state (validated by the authors in [24]) are exploited in this work. For the thick ( $R_{vox} = 2.45$ ), thin ( $R_{vox} = 1.7$ ), and ultra-thin ( $R_{vox} = 7.7$ ) tow systems, a mean resin pocket VF of 4.7%, 2.64%, and 1% were reproduced, respectively. Then, a modified 3D-RSA and deposition strategies are used to generate the plate. The full deposition domain to generate the plate is chosen according to the size of the required virtual sample for the analysis. When working with SVEs, a deposition domain larger than the SVE of interest is used, which is specified in the in-plane as  $ml_t \times ml_t$  (or simply by the side length  $ml_t$ ), where  $m$  is a (side) factor based on the tow length  $l_t$ . During deposition, the draping algorithm accounts for the tow interactions, producing the resin pockets and the out-of-plane FOD ( $\varphi$ ).
- **Sampling of statistical volume elements (SVEs):** the mesostructure generator is employed for producing a number of independent virtual realisations from which SVEs are sampled. The following SVE sizes (defined by the SVE side length  $ml_t$ ) have been shown to reduce the computational cost while obtaining adequate mean values of the elastic properties [24]:  $0.5l_t$  for the thick and thin cases, and  $0.25l_t$  for the ultra-thin case. These sizes are used unless otherwise stated for other analyses.
- **Computational homogenisation of elastic properties:** the voxelised model of the plate defines directly the FE mesh, and the material models are specified according to Table 2, thus building the FE model. Eight-node fully integrated continuum elements are implemented for both materials. Computational homogenisation using periodic boundary conditions is performed in Abaqus [25] to predict the elastic properties of the TBDC plate. The procedure is repeated for each virtual realisation.

- **Statistical analysis of predicted properties:** given the total number of realisations, the following quantities are considered for the statistical and convergence study,

$$\mu = \frac{1}{N_{sim}} \sum_{i=1}^{N_{sim}} a_i, \quad (1)$$

$$S = \sqrt{\frac{1}{N_{sim} - 1} \sum_{i=1}^{N_{sim}} |a_i - \mu|^2}, \quad (2)$$

$$CV = \frac{S}{\mu}, \quad (3)$$

$$\mu_n^{CA} = \frac{1}{n} \sum_{i=1}^n a_i, \quad (4)$$

$$S_n^{CA} = \sqrt{\frac{1}{n-1} \sum_{i=1}^n |a_i - \mu_n^{CA}|^2}, \quad (5)$$

$$(\epsilon_{abs})_n^{CA} = \frac{z_{CI} S_n^{CA}}{\sqrt{n}}, \quad (6)$$

$$(\epsilon_{rel})_n^{CA} = \frac{z_{CI} S_n^{CA}}{\mu_n^{CA} \sqrt{n}}, \quad (7)$$

where  $\mu$ ,  $S$ , and  $CV$  are the mean value, the standard deviation, and the coefficient of variation of the predicted properties  $a_i$  for the total number of independent realisations  $N_{sim}$  required for convergence. Convergence is assessed by computing the absolute and relative errors ( $\epsilon_{abs}$  and  $\epsilon_{rel}$ ) based on the cumulative values (CA) of the mean and standard deviation for a given number of realisations  $n$  of the SVEs. An error of 5% or less is considered suitable, which corresponds to a 95% confidence interval (CI) with  $z_{CI} = 1.96$ . Mean values of the properties are reported.

The limitations and sources of uncertainty of the modelling approach are discussed in the authors' previous work [24]. Aspects such as local compaction and resin bleeding during moulding are not directly considered. An important source of uncertainty is due to the cured tow properties. Additionally, realistic draping ratios must be considered to calibrate the model based on the mesostructure observed in the microscopic images for a given tow system, as in [24]. The model calibration was validated for three representative TBDCs encountered in the literature, covering thick, thin, and ultra-thin tow systems.

**Table 3**

Three baselines for the parametric studies: thick, thin, and ultra-thin tow material systems. The properties are used as inputs in the FE model of TBDCs.

TBDC material system	Tow properties						Plate properties		
	$t_i$ mm	$l_i$ mm	$w_i$ mm	AR $l_i/w_i$	$E_1$ GPa	$E_2$ GPa	$t_p$ mm	VF of resin pockets (%)	In-plane FOD
Thick	0.285	50	8	6.25	131	9	2	4.7	Random
Thin	0.164	50	8	6.25	131	9	2	2.64	Random
Ultra-thin	0.0214	50	8	6.25	131	9	2	1	Random

**Table 4**

Simulation campaign for the parametric studies, performed on the three baselines (thick, thin, and ultra-thin tow cases) specified in Table 3.

Analysis	Study	Parameter	Unit	Variation	Result
Effect of tow design	1	Tow modulus $E_1$	GPa	130–250	$E$ , $G$
	2	Tow thickness $t_i$	mm	0.0214, 0.164, 0.285	FOD $\varphi$
	3	Tow length $l_i$ (or AR)	mm	8–60	$E$ , $G$
Effect of plate design	4	In-plane size (as SVE side length) <sup>a</sup>	–	$0.5l_i$ – $4l_i$	$E$ , $G$
	5	Thickness (as tows number) <sup>a</sup>	–	2–7	$E$ , $G$
	6	In-plane FOD $\theta$	–	Random and preferred cases	$E_x$ , $E_y$ <sup>b</sup>

<sup>a</sup> Plate size is given relative to tow dimensions, as a side length for the in-plane dimensions, and as a number of tows through the thickness of the plate.

<sup>b</sup> Anisotropic case due to preferred in-plane FOD.

### 2.2.3. Parametric study, outputs and sensitivities

Based on material parameters found in the literature (Table 1), manufacturers' data (e.g. [9,10,21]), and practical considerations outlined subsequently, different cases for the parametric study are considered. In particular, two main types of sensitivity analysis methods are considered, namely one-at-a-time ("one way") parametric analysis [26] and scenario analysis, respectively. In the former case, a single model parameter is varied within a selected range, while in the latter a specific combination of interest of the parameters is evaluated. To investigate an extended design space, three baselines are independently used to assess the effect on different material systems, covering thick, thin, and ultra-thin tow cases. This allows to take into account realistic physical changes inherent to the mesostructure that are of practical interest. The baselines specifications of the tow and plate designs are provided in Table 3.

Table 4 summarises the proposed simulation campaign, where both the tow and plate designs are considered. The primary outputs of interest are the statistical mean values of the homogenised elastic properties of the TBDC plate, which can have an isotropic or anisotropic in-plane response depending on the in-plane FOD. The different analyses are generally applied to the three baselines (thick, thin, and ultra-thin tow cases).

In order to study the effect of the tow design, the tow length  $l_i$  (or equivalently the in-plane aspect ratio  $l_i/w_i$ ), and the tow elastic properties are independently varied for each baseline (i.e. one-at-a-time analysis). To design the simulation campaign, important considerations and design constraints are drawn from the state of the art (Table 1) and commercial TBDC materials, both related to manufacturing and mechanical requirements.

Conventional TBDCs, such as HexMC<sup>®</sup> M77 (50 × 8 mm), display an in-plane tow aspect ratio of 6.25 [9], compared to ultra-thin tow TBDCs like TeXtreme<sup>®</sup> 360° (40 × 20 mm) with a tow aspect ratio of 2 [10]. Here it is emphasised that for ultra-thin spread tows, the achievable width versus thickness depends on the spread technology. In addition, a trade-off between mechanical performance and good drapability in the mould is required, which limits the maximum length of the tows. Based on this, the tow length is studied in the range 8–60 mm, which corresponds to aspect ratios 1–8.75.

In terms of mechanical properties,  $E_1$  for standard carbon fibre tows is around 130 GPa (see Table 1), and around 200 GPa or higher for high-modulus carbon fibre ultra-thin spread tows [24]. Typical values of  $E_2$  are found in the range 7–13 GPa. Accordingly, these reference

values are used to set the ranges in Table 4, i.e. 130–250 GPa for  $E_1$ . As a separate scenario analysis, the resulting out-of-plane FODs produced by the baseline material systems are investigated considering their respective tow thicknesses.

At the plate level, three aspects are generally important for its design, which are the nominal plate dimensions (especially the thickness), the VF of resin pockets, and the FOD (usually random). Different plate thicknesses are typically achieved by stacking preassembled TBDC sheets during moulding, offering flexibility to increase the thickness. Commercial plate thicknesses are around 2 mm [9]. However, conflicting objectives are often found in the design and selection for thin-walled structures. On one side, conventional (thick) TBDC designs have been largely strength-driven, instead of stiffness-driven, and previous studies have shown that their strength increases with plate thickness, for a given constant tow thickness [2]. As a result, thick plates have been investigated (Table 1) in a trade-off between performance and weight. On the other hand, novel TBDCs with ultra-thin spread tows made of high-modulus carbon fibres, offer the possibility to obtain a high stiffness and strength (about +30% more) with reduced plate thicknesses [3]. As such, the objective is to reduce the plate thickness without a significant knockdown.

Attaining lower plate thicknesses is challenging, which may require using thinner tows (e.g. spread tows) or reducing the number of tows through the plate thickness. The latter case requires careful analysis since an insufficient number of tows through the thickness affects its in-plane quasi-isotropic response. For ultra-thin tow TBDCs, in-plane isotropy has been reported to be achieved from 0.5 mm [10]. On the contrary, for thick tow TBDCs, the lower-end of plate thicknesses, and the corresponding implications, have not been fully addressed in the current literature. For this purpose, a one-at-a-time parametric analysis is performed on the plate thickness (in terms of the nominal number of tows through the thickness) to study the necessary thickness to achieve quasi-isotropy. Similarly, the effect of the in-plane size on the quasi-isotropic response is assessed.

Additionally, the resin pocket VF and the in-plane FOD also offer additional degrees of freedom in the design to be considered. For the latter, a scenario analysis is proposed using a realistic preferred in-plane FOD to evaluate its impact on the tensile modulus.

Finally, the sensitivities are expressed in terms of percentage changes from a baseline, or as a knockdown with respect to a reference value, as described later.

### 3. Results and discussion

This section investigates the elastic response of TBDC plates via the computational homogenisation of voxel-based FE models for the three material systems (thick, thin, and ultra-thin tow cases) specified in Table 3. The effect of design parameters at the tow and plate levels are presented in Sections 3.1 and 3.2, respectively.

#### 3.1. Tow design parameters

##### 3.1.1. Effect of the longitudinal tow modulus

Four different models are used to investigate the effect of the longitudinal tow modulus  $E_1$ , and to compare the resulting trends.<sup>1</sup> These are an equivalent short-fibre composite model, Cox–Krenchel's model [27], an equivalent laminate (EL) model, and the voxel-based FE model from [24] described in Section 2.2.2. Out of these, the latter is considered the most accurate and the one upon conclusions are drawn, whereas the other three are provided as comparison.

First, treating the material as a short-fibre composite with randomly oriented fibres in the plane, the in-plane moduli  $E_{shortfibre}$  and  $G_{shortfibre}$  of the plate can be predicted by the empirical equations [28]

$$E_{shortfibre} = \frac{3}{8}E_1 + \frac{5}{8}E_2, \quad (8)$$

$$G_{shortfibre} = \frac{1}{8}E_1 + \frac{1}{4}E_2, \quad (9)$$

where  $E_1$  and  $E_2$  are the longitudinal and transversal tow moduli, respectively.  $E_2$  is fixed in this case at the baseline value (9 GPa). The applicability of Eqs. (8) and (9) to TBDCs has been explored in the literature [3]. The second model is Cox–Krenchel's model [27]:

$$E_c = E_m(1 - V_f) + E_f V_f n_l n_o, \quad (10)$$

$$n_l = 1 - \frac{\tanh(\beta l/2)}{\beta l/2}, \quad (11)$$

$$\beta = \frac{1}{r_f} \sqrt{\frac{2G_m}{E_f \ln\left(\sqrt{\frac{\pi/4}{V_f}}\right)}}, \quad (12)$$

where  $E_c$  is the tensile modulus of the composite,  $n_l$  is the length efficiency factor, and  $n_o$  is the orientation factor, which is 0.375 for a random distribution in the plane [29]. The tensile and shear moduli ( $E_m$ ,  $G_m$ ) of the matrix are given in Table 2. The fibre length  $l$  corresponds to the baseline of the tow length 50 mm, and the fibre diameter  $r_f$  is assumed to be 5  $\mu\text{m}$  considering typical values [30]. The fibre volume fraction in the tows  $V_f$  is extracted from the virtual voxel models, accounting for the resin pocket VF and the volume fraction of tows. To consider the effect of modulus  $E_1$ , the rule of mixtures is applied to the tow to back-calculate the modulus  $E_f$ .

Thirdly, an EL model with a quasi-isotropic lay-up [45/−45/90/0]<sub>s</sub> is used. Classical lamination theory (CLT) [31] is used to predict the elastic response of the laminate, where all laminae are assumed to have perfect bonding and where the laminae properties correspond to the tow properties. The effective elastic properties are computed from the compliance matrix. Lastly, the fourth model corresponds to the voxel-based FE model with computational homogenisation as described in Section 2.2, which is of primary interest in this work. For the latter, mean values of the moduli are reported.

The predicted plate moduli are shown in Fig. 3. In general, all cases exhibit an increasing trend of the in-plane plate moduli  $E$  and  $G$  with respect to the modulus  $E_1$ , approximately with a linear behaviour. The short-fibre model, Cox–Krenchel's model (on lower end), and the EL

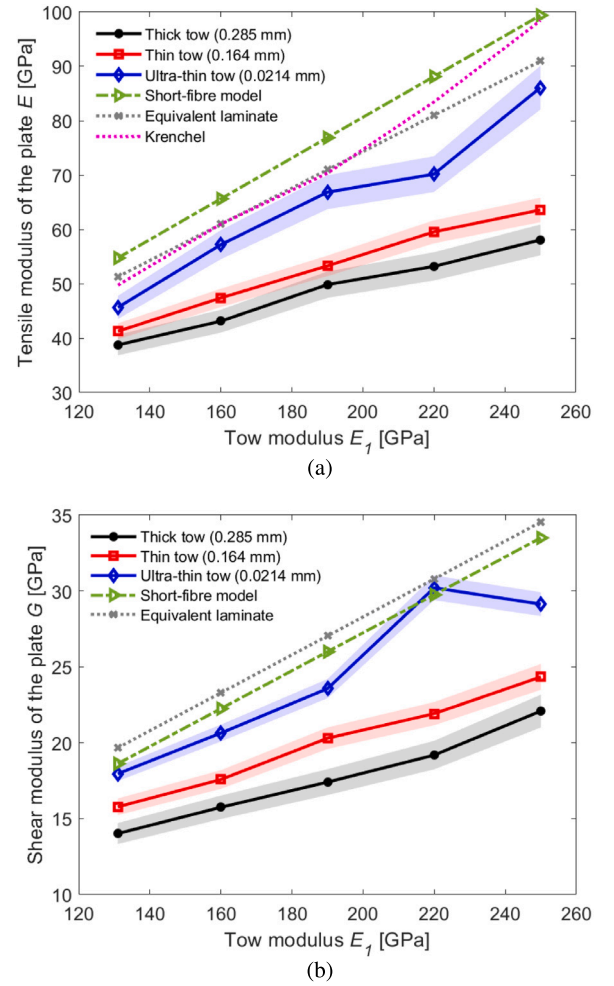


**Fig. 3.** Effect of the longitudinal tow modulus  $E_1$  on the in-plane plate moduli ( $E$ ,  $G$ ) for three TBDC material systems, and comparison with short-fibre and equivalent laminate models. Data points predicted by the FE model for thick, thin, and ultra-thin cases correspond to the mean values. Shaded regions show the 95% confidence intervals (CI). Other parameters are fixed to the baseline values given in Table 3. (a) Tensile modulus  $E$ , (b) Shear modulus  $G$ .

model all predict a trend with a similar slope, presenting a higher sensitivity to  $E_1$  compared to that obtained by the FE model. Moreover, the latter predicts a less sensitive response for the thick and thin tow cases, in contrast to the ultra-thin tow case. For instance, a 10% increase in  $E_1$  relative to the baseline value (131 GPa) results in the following increase in  $E$ , approximated by local linearisation, according to each case: short-fibre model (9%), Cox–Krenchel's model (10.2%), EL (8.5%), thick (5.1%), thin (6.7%), and ultra-thin (11.4%). Similarly, the predicted changes for the shear modulus  $G$  are: short-fibre model (7.4%), EL (8.3%), thick (5.6%), thin (5.2%), and ultra-thin (6.9%). These differences are attributed to the resin pockets VF and the out-of-plane FOD, which vary between the thick, thin, and ultra-thin tow systems (Section 2.2). The out-of-plane FODs are further explored in Section 3.1.2. In contrast to the used FE model, short-fibre and EL models do not take these aspects into account.

In addition, it is observed that the values predicted by the short-fibre model, Cox–Krenchel's model, and EL model are considerably higher than those predicted by the FE model, independent of the material system. The short-fibre model does not account directly the fibre length and aspect ratio, overpredicting the modulus compared to Cox–Krenchel's model. Furthermore, due to the different slopes of the trends, this difference is greater for ultra-high modulus tows (e.g. 240

<sup>1</sup> The relatively limited effect of  $E_2$  is illustrated in Section 3.1.4 and thus excluded from further analysis.

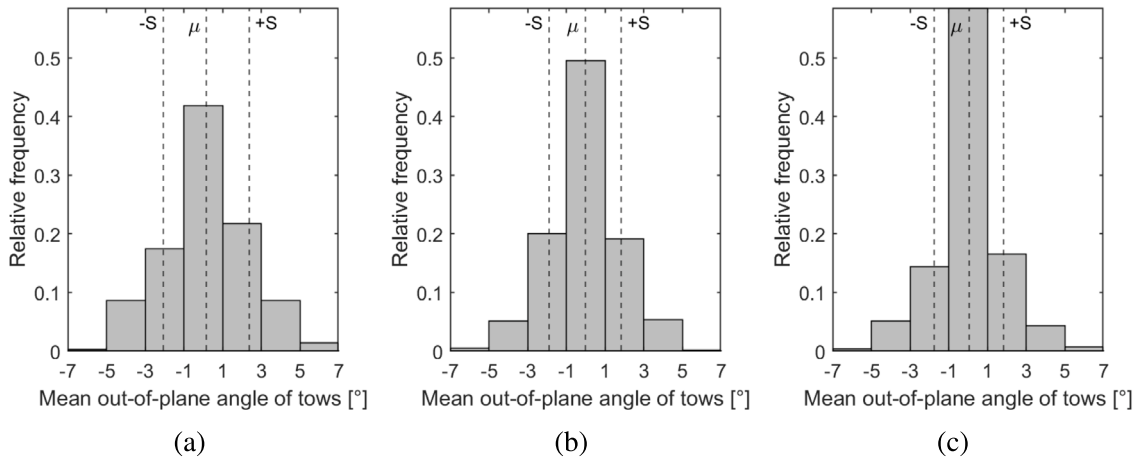


**Fig. 4.** Effect of the tow thickness on the out-of-plane FOD for three TBDC material systems. Other parameters are fixed to the baseline values given in Table 3. (a) Thick tow 0.285 mm, (b) Thin tow 0.164 mm, (c) Ultra-thin tow 0.0214 mm. The mean value  $\mu$  and the standard deviation  $S$  are indicated.

GPa or higher) compared to more conventional or moderately high-modulus tows (e.g. 130 GPa). The deviation is even more pronounced for material systems with thicker, ultra-high modulus tows, displaying a difference in stiffness prediction between the FE model and all the other (approximate) models of up to 70%. This illustrates the clear benefit of using the proposed FE model since it allows to incorporate actual mesostructural effects of TBDCs in the elastic predictions.

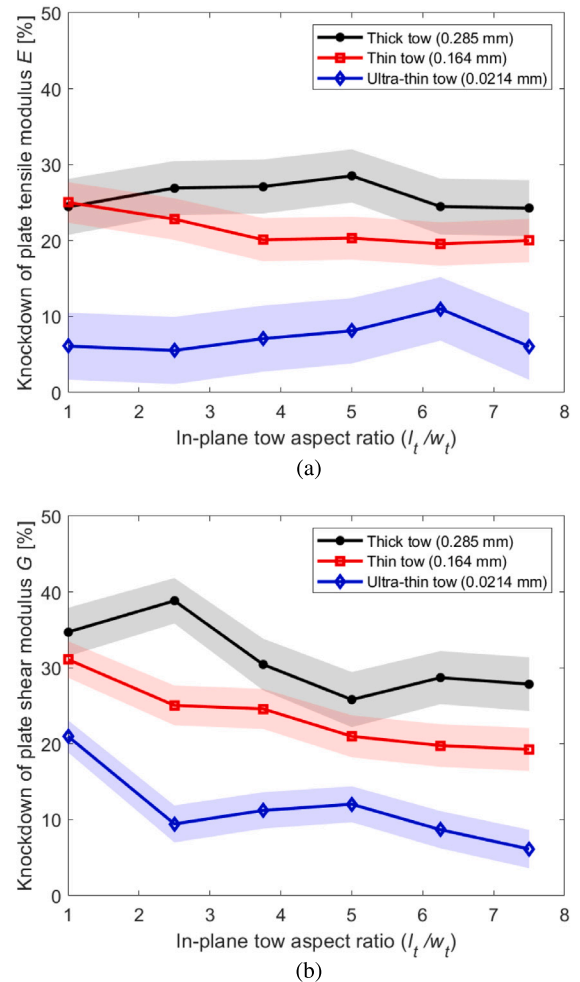
### 3.1.2. Effect of the tow thickness on the out-of-plane FOD

Fig. 4 shows how the tow thickness affects the statistical distribution of the out-of-plane angles of the tows in the plate mesostructure. It is observed that in the thick tow system, 41.8% of the tows have a mean out-of-plane angle between  $-1^\circ$  and  $1^\circ$ , while in the thin and ultra-thin tow systems the corresponding amounts are 49.6% and 58.4%, respectively. This indicates that an additional 8% of the total number of tows in the thick system have mean out-of-plane angles outside the range  $-1^\circ$  and  $1^\circ$ , compared to the thin tow system. The latter 8% contributes to the width of the statistical distribution of the mean out-of-plane angles of the thick tow system, especially in the range  $3-5^\circ$  (including the corresponding negative angles), reaching a total of 17.2% in the given range, which is larger than in thinner systems. A similar difference of 8% is observed between the thin and ultra-thin tow systems. Therefore, the tow thickness clearly affects the crimp of the tows thereby also the resulting moduli of the plates. From the manufacturing viewpoint, the resulting statistical distribution of the out-of-plane angles largely depends on the compaction level required for the consolidation of the material during compression moulding [23]. Thus, the applied pressure is a way of controlling the out-of-plane FOD.

### 3.1.3. Effect of the in-plane tow aspect ratio

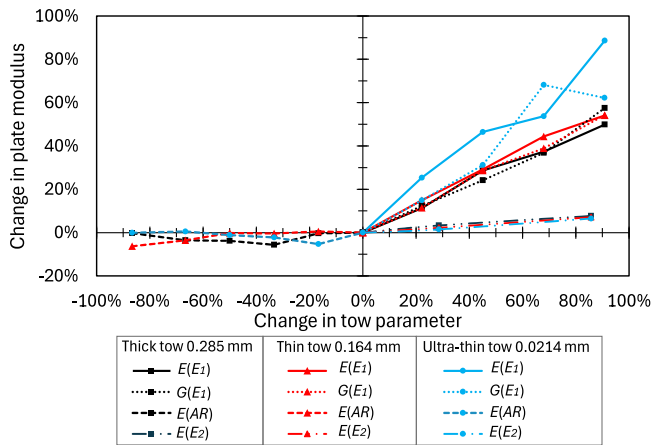
In this section, the effect of the in-plane aspect ratio of the tows ( $l_t/w_t$ ) is investigated by changing the tow length  $l_t$  while fixing the tow width  $w_t$  at the baseline value in Table 3. To enable a comparison between the three material systems, the mean value of the moduli resulting from changes in tow aspect ratio are normalised by computing the knockdown with respect to the EL model with a quasi-isotropic lay-up  $[45/-45/90/0]_s$ . For instance, the knockdown in the mean tensile modulus  $E$  is computed by  $|E - E_{EL}|/E_{EL}$ . Similarly, for the mean shear modulus  $G$ , the knockdown is given by  $|G - G_{EL}|/G_{EL}$ .

Fig. 5(a) shows the knockdown in the mean tensile modulus  $E$  due to the in-plane aspect ratio of the tow. For the three material systems under study, no clear general trend is found. The relative change can be considered to be small for the analysed aspect ratios, being around 5% or less. For thick tow systems, this is in line with experimental



**Fig. 5.** Effect of the in-plane tow aspect ratio on the knockdown of the plate moduli for three TBDCs. The tow length  $l_t$  is used to change the aspect ratio, and other parameters are fixed to the values in Table 3. Data predicted by the FE model for thick, thin, and ultra-thin cases correspond to mean values. Shaded regions show the 95% confidence intervals (CI). (a) Tensile modulus  $E$ , (b) Shear modulus  $G$ .





**Fig. 6.** Sensitivity analysis of the plate moduli ( $E$ ,  $G$ ) versus tow parameters ( $E_1$ ,  $E_2$ ,  $AR$ ) for three TBDCs. Data points predicted by the FE model correspond to the mean values. Other parameters are fixed to the baseline values given in Table 3. The zero reference (0%) for tow parameters are: 131 GPa for  $E_1$ , 7 GPa for  $E_2$ , and 7.5 for aspect ratio ( $AR$ ).

observations [17]. For the thin tow system the trend may appear to be more clear, albeit with small changes. This can be attributed to the fact that the thick tow system have a higher variability that can outweigh the trend, while thinner systems have less variability.

Fig. 5(b) shows the knockdown in the mean shear modulus  $G$ . Contrary to the tensile modulus, all three systems show a reduction in the knockdown as the in-plane aspect ratio of the tow increases. In this case, the relative change between the extreme values is close to 10%, which is significant. The trend is consistent with experimental studies reported in the literature for moderately thin tow systems [17]. The present study shows that the response is similar also for thick and ultra-thin tow systems. Since each material system presents comparable statistical ranges for the volume fraction of resin pockets for the different tow aspect ratios, and the sampling of statistical volume elements accounts for the aspect ratio through the tow length (Section 2.2.2), the observed effect may be attributed primarily to the stress-transfer between tows. This is further supported by the length efficiency factor in Eq. (11) from Cox-Krenchel's model, which also suggests a knockdown linked to the load-transfer when the aspect ratio is reduced.

### 3.1.4. Sensitivity analysis of tow parameters

Fig. 6 summarises and compares the sensitivities of the three material systems for the different tow parameters. For the longitudinal tow modulus  $E_1$ , the lowest value 131 GPa was used as the zero reference, thus percentage changes in modulus correspond to an increase. For the in-plane aspect ratio ( $AR$ ), the largest value 7.5 was used as the zero reference, and percentage changes in aspect ratio correspond to a decrease. Additionally, the sensitivity to the tow transverse modulus  $E_2$  was investigated (zero reference is 7 GPa).

The sensitivities obtained in Fig. 6 highlight the previous findings. It shows a low sensitivity of the plate moduli to the in-plane aspect ratio (modulus change of  $-6.3\%$  for a change of  $-87\%$  in  $AR$  from the reference value 7.5), and a high sensitivity to the tow longitudinal modulus  $E_1$  (a modulus change in the range of  $50\%$ – $90\%$ , depending on the tow system, for a change of  $90\%$  in  $E_1$  from the reference value 131 GPa). For the latter, the highest sensitivities are observed in ultra-thin tow systems, which can even be up to twice as high compared to thicker tow systems, depending on the change in the tow modulus. Meanwhile, the sensitivity to the tow transverse modulus  $E_2$  is considerably low (for practical values it is less than  $2\%$ ). This clearly indicates that since the transverse modulus of UD tows is dominated by the matrix properties [31], the effect of  $E_m$  is weak.

## 3.2. TBDC plate design parameters

### 3.2.1. Effect of the plate size on the quasi-isotropic response

The random deposition of tows to generate TBDC plates results in a quasi-isotropic behaviour in the plane, which is of special interest for this materials when compared to laminated composites. However, random orientations also produce a significant variability in their mechanical properties [32]. Kravchenko et al. [19] reported an experimental CV between  $5\%$ – $10\%$ . Higher values, between  $13\%$ – $18\%$ , have also been measured [2,33]. Such values are considered rather high and over the range of what is generally accepted for conventional isotropic materials,<sup>2</sup> for which lower limits are typically used to ensure reliability, structural safety and probabilistic design. Yet, the mesostructural design conditions to ensure this quasi-isotropic behaviour in TBDCs have not been addressed in the literature.

In this section, the following statistically-based numerical approach is proposed to quantify and assess the quasi-isotropic response of TBDCs: (1) the voxel-based mesoscale FE model is used to explicitly incorporate the tow and plate design dimensions and properties of concern; (2) several realisations of SVEs are generated and virtually tested using computational homogenisation; (3) a statistical analysis is performed to determine the convergence of the descriptors  $\mu$ ,  $S$ , and  $CV$  of the mechanical properties; (4) the statistical variation in the material properties is evaluated based on the CV, by comparing it with a quasi-isotropy criterion (CV below a given threshold) for the corresponding material system. Together with the difference in directional properties, the CV can be used to assess whether a quasi-isotropic or anisotropic behaviour is exhibited. In this study, it is of interest to apply this methodology to identify possible design constraints in TBDCs, for example critical minimum plate dimensions to guarantee quasi-isotropy at the macroscale, both through the thickness and in the plane (Fig. 7). Thus, the proposed methodology is repeated for different plate sizes.

To establish a criterion for assessing the quasi-isotropy of TBDCs, experimental values of CV reported in the literature are considered. Specifically, Kravchenko et al. [19] tested 67 samples of TBDC plates with thin tows and several plate thicknesses, with an average CV between coupons of  $8.17\%$ . For ultra-thin tows, Katsivalis et al. [3] carried tensile tests on 12 samples, obtaining a mean tensile modulus of  $69.95$  GPa, with a standard deviation of  $3.23$  GPa and a CV of  $4.61\%$ . Since these two material systems are of key relevance in practice, their average value  $6.39\%$  is indicative for moderately thin tow TBDCs. Accordingly, a rounded CV of  $6\%$  is chosen as a suitable criterion in this study.

Fig. 8 presents the distributions of the tensile modulus of the plate for three SVEs with different in-plane sizes for the thick tow system (with a nominal number of tows through the thickness of 7). The thick tow system is used as a prototype case to reduce the computational cost [24], and the same trend is representative for all three material systems. The in-plane dimensions of the SVE are specified by the SVE side length  $ml_t$  relative to the tow length  $l_t$ , where  $m$  is the SVE side factor. For each SVE size, simulations were performed until statistical convergence was reached, and the obtained CV is reported. In Fig. 8, it is observed that the width of the distribution reduces when the in-plane size increases. Fig. 9 shows the corresponding effect of the in-plane SVE size on the variability (CV) of the tensile modulus. From Fig. 9, an in-plane plate size of around three times the tow length (SVE side length  $3l_t$ ) is sufficient to obtain a quasi-isotropic behaviour, given the defined limit of  $CV \leq 6\%$ . This size can be considered as the critical minimum size in the plane to obtain a quasi-isotropic macroscale response.

The same statistical-based approach can be used to assess the effect of the plate thickness, or equivalently the nominal number of tows

<sup>2</sup> It is of interest to note that the typical CV of metals as structural steels have been reported ranging up to  $6\%$ – $13\%$  [34], where lower values are more conservative.

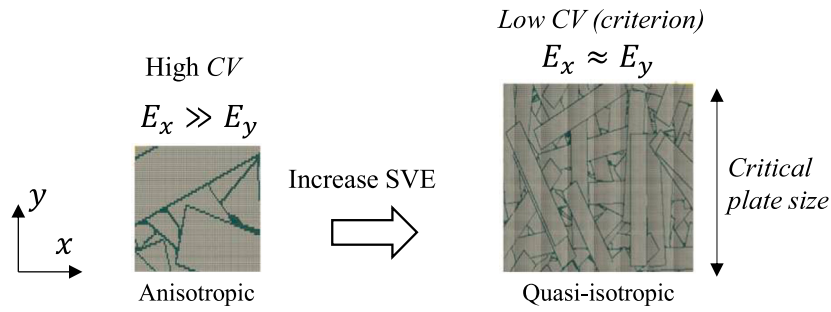


Fig. 7. Statistical approach to assess quasi-isotropy in TBDC plates. In-plane view is shown through representative FE models of TBDCs used in Abaqus.

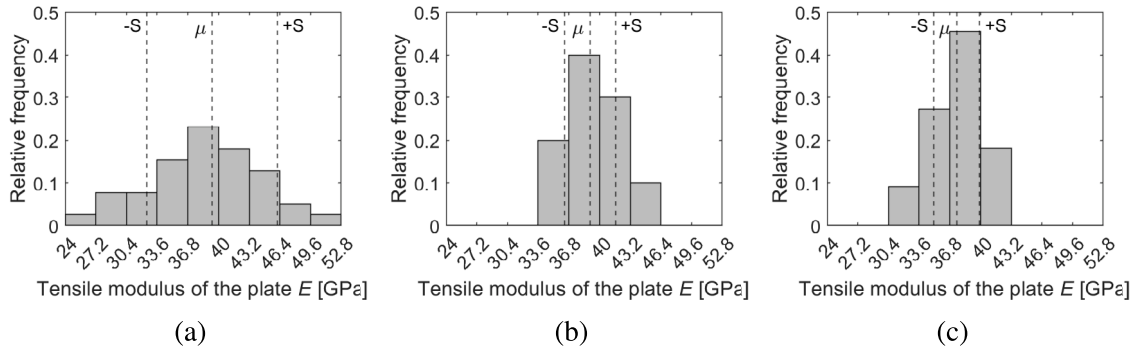


Fig. 8. Effect of the in-plane SVE size, specified by the SVE side length relative to the tow length  $l_t$ , on the distribution of the plate tensile modulus  $E$  for the prototype case (thick tow system). Other parameters are fixed to the baseline values in Table 3. (a) SVE side length  $0.5l_t$ , (b) SVE side length  $1.5l_t$ , (c) SVE side length  $3l_t$ . The mean value  $\mu$  and the standard deviation  $S$  are indicated.

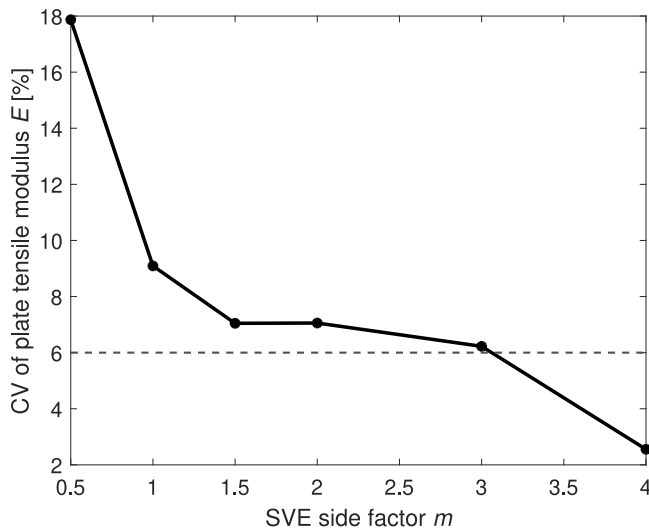


Fig. 9. Effect of the in-plane SVE size, specified as a factor of the tow length  $l_t$ , on the CV of the plate tensile modulus  $E$  for the prototype case (thick tow system). Other parameters are fixed to the baseline in Table 3. Criterion for 6% CV is indicative.

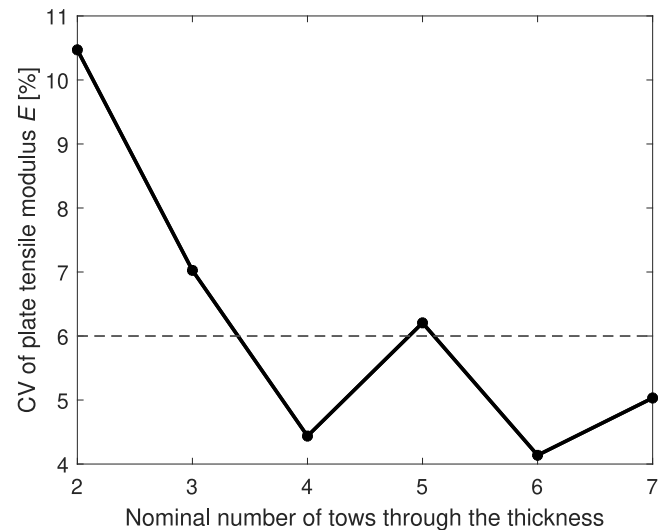
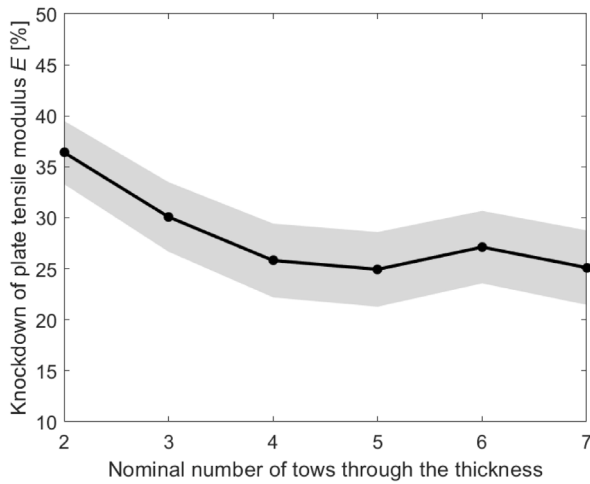


Fig. 10. Effect of the nominal number of tows through the thickness on the CV of the plate tensile modulus  $E$  for the prototype case (thick tow system). In-plane size is fixed (SVE  $3l_t$ ). Other parameters are fixed to the baseline in Table 3. Criterion for 6% CV is indicative.

through the thickness, on the quasi-isotropic response, while the in-plane size of the plate is fixed. Based on Fig. 9, the in-plane size is chosen with an SVE side length of  $3l_t$ . Similar to Fig. 7, the CV and statistical distribution of the tensile modulus are studied for different plate thicknesses. When the plate thickness is reduced, both the width of the distribution and the CV of the tensile modulus increase, as shown in Fig. 10. It is observed that at least 4 tows through the thickness are sufficient to produce a quasi-isotropic behaviour, given the  $CV \leq 6\%$  limit.

In contrast to the in-plane sizing, thickness sizing has further implications for the plate modulus. To analyse this, the knockdown of the mean tensile modulus with respect to the EL model is obtained, as presented in Fig. 11. It is observed that below 4 tows through the thickness, the modulus is considerably reduced, between 5%–10%. This behaviour is attributed to the fact that as the number of tows through the thickness decreases, the real distribution of the in-plane angles of the tows does not attain enough tows in the required directions to generate a corresponding high stiffness in the plate. Therefore, a



**Fig. 11.** Effect of the nominal number of tows through the thickness on the plate tensile modulus  $E$  for the prototype case (thick tow system). In-plane size is fixed ( $SVE\ 3l_t$ ). Other parameters are fixed to the baseline in Table 3. Data correspond to the mean values, and shaded regions show the 95% confidence intervals (CI).

minimum of 4 tows through the thickness can be considered as the critical minimum thickness both to achieve in-plane quasi-isotropy and to avoid a significant knockdown in the modulus.

### 3.2.2. Effect of preferred in-plane FOD of the tows

During the manufacturing of TBDC plates, the fraction of the mould volume initially occupied by tows after deposition (i.e. the charge percentage), affects the material flow during compression moulding. This produces a redistribution of tow orientations, thereby inducing a preferred in-plane FOD. The precharge location and dimensions have been demonstrated to affect the mechanical performance, which may be optimised [35]. In this context, the term “preferred” indicates the direction in which the stiffness is increased by the manufacturing process selection.

In this section, the effect on plate moduli by a preferred in-plane FOD induced with a high-flow condition (corresponding to 40% charge) is studied, based on realistic distributions reported by Sommer et al. [11]. Fig. 12 presents the experimentally determined tow orientation distribution obtained from [11], together with a kernel distribution fit (blue curve) of this data used as input in the voxel-based FE mesoscale generator. Here, the preferred orientation of  $0^\circ$  corresponds to the  $x$ -direction. Fig. 13 compares the tow orientations with preferred FOD and random FOD for the TBDC in [11] used as reference.

First, the implementation of the FOD in the modelling methodology is validated by comparing the results predicted by the mesoscale generator for the reference TBDC in [11], as shown in Table 5. The material properties for the tows are provided in [36]. For the reference TBDC, Sommet et al. [11] reported  $E_x = 56.5$  GPa and  $E_y = 28.3$  GPa, with a ratio  $E_x/E_y = 2$ . The predicted mean values in this study are in good agreement, which are  $E_x = 52.45$  GPa,  $E_y = 30.63$  GPa, and  $E_x/E_y = 1.71$ . As expected, the behaviour is henceforth anisotropic for the preferred in-plane FOD.

Finally, the same preferred in-plane FOD is applied as input to the three baseline material systems of this study, as compared in Table 5. As illustration, Fig. 14 shows the convergence of the CA of moduli  $E_x$  and  $E_y$  in 10 virtual realisations for the thick tow TBDC. Now, the ratios of the moduli give a value of around 2 for all three material systems. Also, comparing the resulting  $E_x$  and  $E_y$  with preferred FOD and the corresponding quasi-isotropic tensile modulus  $E$  (random FOD), gives ratios of around 1.5 and 0.7, respectively. This indicates a 50% gain in  $E_x$  by controlling the designed FOD, while there is a decrease in  $E_y$  by 30%.

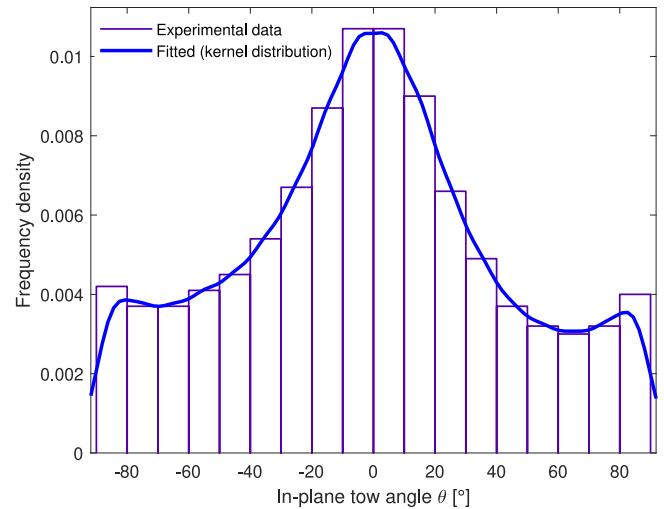


**Fig. 12.** Data of an experimentally obtained preferred in-plane FOD from [11], and a kernel distribution (blue curve) fitted to the data used as input in the voxel-based mesoscale generator.

## 4. Conclusions

The present work uses a numerical framework to investigate the effects of mesostructural parameters on the macroscopic elastic properties of TBDCs. A novel 3D voxel-based FE model together with a statistical analysis of SVEs is exploited to incorporate parameters both at the tow and plate levels for an extended design space, including thick, thin and ultra-thin tow systems. The simulation campaign comprises several parametric analyses, and the results show opportunities to optimise and tailor the stiffness of TBDCs plates depending on the type of tows used and how they are distributed in-plane. The conclusions are summarised here:

- **Tow moduli:** An approximately increasing linear trend has been observed between the longitudinal tow modulus  $E_1$  and the in-plane quasi-isotropic tensile modulus  $E$  of the plate, where the sensitivity depends on the mesostructures characteristics. Ultra-thin tow systems are found to be almost twice as sensitive to the value of  $E_1$  as thicker systems. This is attributed to the fact that the increased VF of resin pockets and the increasing amount of tows oriented out-of-plane lead to a more significant decrease in the elastic properties of the latter. Thus, the use of ultra-high modulus tows offers greater opportunities to improve the performance of ultra-thin tow systems. As a consequence, if the aim is to obtain a stiffer material, it is more beneficial to first decrease the thickness of the tows before changing to a high-modulus fibre. Several conditions in the manufacturing process must be considered to achieve this. The pre-impregnated tow thickness can be controlled by the number of fibre filaments in the tow, their resin content, or by redistributing their packing using spreading technology. Then, compression moulding also affects the cured thickness of the tows. It has recently been shown that by carefully designing the manufacturing process, engineering-relevant (high enough) fibre volume fractions can be achieved also for ultra-thin TBDCs [3]. Regarding the tow transverse modulus  $E_2$ , a low sensitivity was found for all cases. Furthermore, it is evident that simplified models such as ELs, short-fibre models, and Cox–Krenchel’s model have limitations in predicting the properties of thicker tow systems, considering the significant over-predictions of elastic moduli. This is especially critical when using ultra-high modulus tows in thick systems. Additionally, since tow dimensions and interactions are not directly

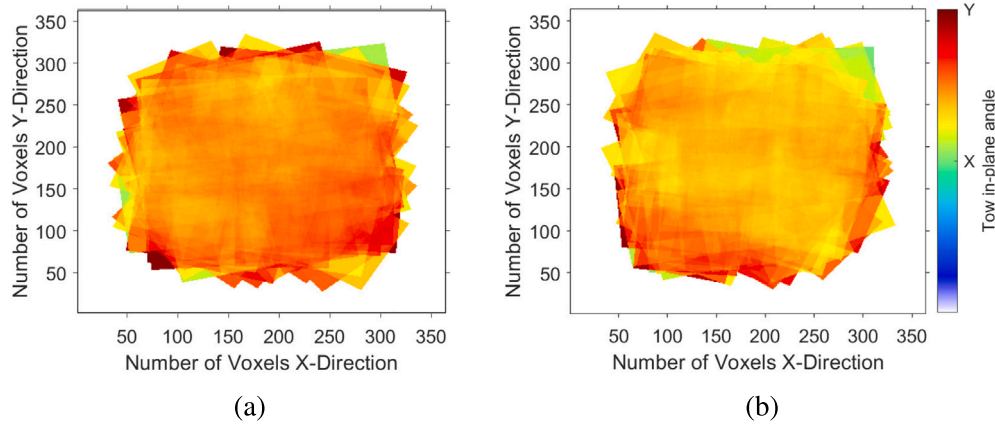


**Fig. 13.** Top view of TBDC plates showing the tow orientations with two different in-plane FODs for the reference TBDC. Tow angles are colour-mapped, such  $x$  and  $y$  directions correspond to  $0^\circ$  (green) and  $90^\circ$  (red). (a) Random FOD, (b) Preferred FOD producing anisotropy.

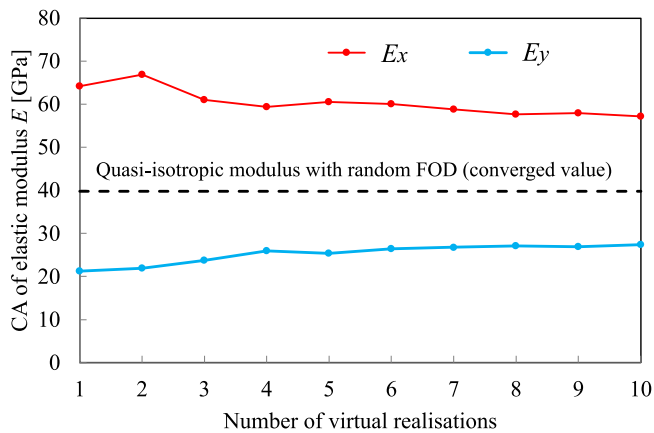
**Table 5**

Plate moduli for several material systems with preferred in-plane FOD. Mean values are reported.

Case	Description	$E_x$ (GPa)	$E_y$ (GPa)	$E_x/E_y$	$E_x/E$	$E_y/E$
Reference TBDC <sup>a</sup>	Experimental data from [11]	56.5	28.3	2.0	1.42	0.71
Reference TBDC <sup>a</sup>	Predicted for validation	52.45	30.63	1.71	1.36	0.79
Thick tow TBDC <sup>b</sup>	Predicted by FE model	57.19	27.41	2.09	1.48	0.71
Thin tow TBDC <sup>b</sup>	Predicted by FE model	61.30	30.09	2.03	1.49	0.73
Ultra-thin tow TBDC <sup>b</sup>	Predicted by FE model	68.36	33.39	2.05	1.50	0.73

<sup>a</sup> Reference TBDC with preferred FOD [11]. Tow dimensions are  $12.7 \times 12.7 \times 0.14$  mm.

<sup>b</sup> Prediction for baselines of this study with preferred FOD, and comparison with quasi-isotropic tensile modulus  $E$  (random FOD). Other parameters are fixed as in Table 3.



**Fig. 14.** Convergence of the cumulative average (CA) of the anisotropic plate moduli  $E_x$  and  $E_y$  for the thick tow TBDC with preferred FOD, and comparison with the converged quasi-isotropic modulus  $E$  (random FOD).

accounted for (in contrast to the voxel-based FE-models), the use of such analytical models is limited in material architecture optimisation.

- **In-plane tow aspect ratio:** This study shows that there is no clear effect of the in-plane tow aspect ratio on the tensile modulus  $E$  of the plate, for any of the three material systems. On the other hand, there is a more noticeable effect on the shear modulus  $G$ , where each material system experiences a knockdown when the aspect ratio of the tows is reduced. Although from a practical point of view the tensile modulus  $E$  is usually of greater interest, there appears to be opportunities to improve the macroscopic shear response by using tows with a larger aspect ratio.

- **Out-of-plane FOD:** The results show that the width of the out-of-plane angle distribution depends on the tow thickness of the specific material system. In particular, reducing the thickness of the tows also reduces the VF of resin pockets, contributing to the reduction of crimps and out-of-plane angles. This implies that the ultra-thin tow system presents not only a smaller width in the distribution, but also a higher stiffness with less variability, compared to thicker systems.
- **Plate size:** the proposed statistically-based numerical approach enables the assessment of variations in the quasi-isotropic response of the plates. This allows the identification of critical minimum dimensions to ensure a quasi-isotropic response. For the in-plane size, it was found that the in-plane dimensions mainly affect the CV of the elastic properties. It was also found that an in-plane size of at least three tow lengths needs to be considered to obtain a satisfactory in-plane quasi-isotropic response. This is explained by the fact that a reduction of the width of the statistical distributions of elastic properties is obtained for increasing in-plane dimensions. A direct implication of the minimum in-plane size is that if TBDCs are to be considered as quasi-isotropic in design, strains cannot vary substantially (in any direction) over this minimum in-plane length. If strain gradients are pronounced, the material heterogeneity needs to be explicitly considered. Regarding the plate thickness, it affects the variability of properties but also produces a variation in stiffness knockdown, which requires special attention. In the studied range, this detriment can be reduced by considering at least 4 tows through the thickness of the plate. Therefore, this study shows that there are critical minimum dimensions both in thickness and in the plane that must be satisfied.
- **Preferred in-plane FOD of the tows:** Inducing a preferred in-plane FOD during compression moulding results in a TBDC plate with an anisotropic response. The moduli of this anisotropic response can be predicted by the voxel-based FE generator by providing



a realistic in-plane FOD as input. Specific to the case studies, moduli ratios  $E_x/E_y$  result in the range 1.7–2. As expected, this is observed for all three material systems under study. When compared with random FOD, the preferred FOD showed a 50% improvement in  $E_x$ , while  $E_y$  is reduced. This allows directional properties to be considered according to design requirements, which can be achieved by tailoring their manufacturing. Long term, the voxel-based FE generator could be used in a inverse way to obtain the in-plane tow distribution necessary to achieve a desired amount of anisotropy in stiffness properties.

### CRedit authorship contribution statement

**Luis Gulfo:** Writing – original draft, Visualization, Validation, Software, Methodology, Investigation, Formal analysis, Conceptualization. **Ioannis Katsivalis:** Writing – review & editing, Supervision, Investigation, Formal analysis. **Leif E. Asp:** Writing – review & editing, Supervision, Funding acquisition. **Martin Fagerström:** Writing – review & editing, Supervision, Resources, Project administration, Methodology, Conceptualization.

### Declaration of competing interest

The authors declare that they have no known competing financial interests or personal relationships that could have appeared to influence the work reported in this paper.

### Acknowledgements

The competence centre TechForH2 is hosted by Chalmers University of Technology and is financially supported by the Swedish Energy agency (P2021-90268) and the member companies Volvo, Scania, Siemens Energy, GKN Aerospace, PowerCell, Oxeon, RISE, Stena Rederier AB, Johnson Matthey and Inspilorion.

### Data availability

Data will be made available on request.

### References

- [1] Hexcel Corporation, Annual report, 2016.
- [2] M. Alves, D. Carlstedt, F. Ohlsson, L.E. Asp, S. Pimenta, Ultra-strong and stiff randomly-oriented discontinuous composites: Closing the gap to quasi-isotropic continuous-fibre laminates, *Compos. A Appl. Sci.* 132 (2020) 105826.
- [3] I. Katsivalis, M. Persson, M. Johansen, F. Moreau, E. Kullgren, M. Norrby, D. Zenkert, S. Pimenta, L.E. Asp, Strength analysis and failure prediction of thin tow-based discontinuous composites, *Compos. Sci. Technol.* 245 (2024) 110342.
- [4] I. Katsivalis, M. Norrby, F. Moreau, E. Kullgren, S. Pimenta, D. Zenkert, L.E. Asp, Fatigue performance and damage characterisation of ultra-thin tow-based discontinuous tape composites, *Compos. B Eng.* 281 (2024) 111553.
- [5] I. Katsivalis, V. Signorini, F. Ohlsson, C. Langhammer, M. Minelli, L.E. Asp, Hydrogen permeability of thin-ply composites after mechanical loading, *Compos. A Appl. Sci.* 176 (2024) 107867.
- [6] FAA USA, DOT/FAA/TC-16/35 certification of discontinuous fiber composite structures via stochastic modeling, 2017, <https://www.tc.faa.gov/its/worldpac/techrpt/tc16-35.pdf>.
- [7] EASA, AMC-20 amendment 23, 2023, <https://www.easa.europa.eu/en/document-library/easy-access-rules/easy-access-rules-acceptable-means-compliance-airworthiness>.
- [8] M. Tuttle, P. Feraboli, Certification of discontinuous composite material forms for aircraft structures, 2024, [https://www.wichita.edu/industry\\_and\\_defense/NIAR/Documents/W0800\\_UW\\_TuttleFeraboli.pdf](https://www.wichita.edu/industry_and_defense/NIAR/Documents/W0800_UW_TuttleFeraboli.pdf). (Retrieved 2024).
- [9] Hexcel Corporation, HexMC user guide, 2014, [https://www.hexcel.com/user\\_area/content\\_media/raw/HexMC\\_UserGuide.pdf](https://www.hexcel.com/user_area/content_media/raw/HexMC_UserGuide.pdf).
- [10] A.B. Oxeon, Textreme 360° discontinuous fiber composites (DFC), 2024, <https://www.textreme.com/product/360/360-discontinuous-composites>.
- [11] D.E. Sommer, S.G. Kravchenko, B.R. Denos, A.J. Favaloro, R.B. Pipes, Integrative analysis for prediction of process-induced, orientation dependent tensile properties in a stochastic prepreg platelet molded composite, *Compos. A Appl. Sci.* 130 (2020) 105759.
- [12] L.M. Martulli, L. Muyschondt, M. Kerschbaum, S. Pimenta, S.V. Lomov, Y. Swolfs, Carbon fibre sheet moulding compounds with high in-mould flow: Linking morphology to tensile and compressive properties, *Compos. A Appl. Sci.* 126 (2019) 105600.
- [13] C. Nony-Davadie, L. Peltier, Y. Chemisky, B. Surowiec, F. Meraghni, Mechanical characterization of anisotropy on a carbon fiber sheet molding compound composite under quasi-static and fatigue loading, *J. Compos. Mater.* 53 (11) (2019) 1437–1457.
- [14] S.G. Kravchenko, D.E. Sommer, R. Byron Pipes, Uniaxial strength of a composite array of overlaid and aligned prepreg platelets, *Compos. A Appl. Sci.* 109 (2018) 31–47.
- [15] Y. Li, S. Pimenta, J. Singgih, S. Nothdurfter, K. Schuffenhauer, Experimental investigation of randomly-oriented tow-based discontinuous composites and their equivalent laminates, *Compos. A Appl. Sci.* 102 (2017) 64–75.
- [16] P. Feraboli, E. Peitso, F. Deleo, T. Cleveland, P.B. Stickler, Characterization of prepreg-based discontinuous carbon fiber/epoxy systems, *J. Reinf. Plast. Compos.* 28 (10) (2009) 1191–1214.
- [17] M. Selezneva, L. Lessard, Characterization of mechanical properties of randomly oriented strand thermoplastic composites, *J. Compos. Mater.* 50 (20) (2016) 2833–2851.
- [18] M. Alves, S. Pimenta, The influence of 3D microstructural features on the elastic behaviour of tow-based discontinuous composites, *Compos. Struct.* 251 (2020) 112484.
- [19] S.G. Kravchenko, D.E. Sommer, B.R. Denos, A.J. Favaloro, C.M. Tow, W.B. Avery, R. Byron Pipes, Tensile properties of a stochastic prepreg platelet molded composite, *Compos. A Appl. Sci.* 124 (2019) 105507.
- [20] S. Ko, T. Nakagawa, Z. Chen, W.B. Avery, E.J. Adams, M.R. Soja, M.H. Larson, C.Y. Park, J. Yang, M. Salviato, Effects of average number of platelets through the thickness and platelet width on the mechanical properties of discontinuous fiber composites, *Compos. A Appl. Sci.* 177 (2024) 107945.
- [21] Toray Composite Materials America, Inc., 2510 prepreg system data sheet, 2020.
- [22] Y. Li, S. Pimenta, Development and assessment of modelling strategies to predict failure in tow-based discontinuous composites, *Compos. Struct.* 209 (2019) 1005–1021.
- [23] D.E. Sommer, S.G. Kravchenko, R. Byron Pipes, A numerical study of the meso-structure variability in the compaction process of prepreg platelet molded composites, *Compos. A Appl. Sci.* 138 (2020) 106010.
- [24] L. Gulfo, O. Haglund Nilsson, J. Sjöberg, I. Katsivalis, L.E. Asp, M. Fagerström, A 3D voxel-based mesostructure generator for finite element modelling of tow-based discontinuous composites, *Compos. B Eng.* 278 (2024) 111405.
- [25] Dassault Systèmes Simulia Corp., Abaqus/CAE user's guide, 2022.
- [26] A. Saltelli, M. Ratto, T. Andres, F. Campolongo, J. Cariboni, D. Gatelli, M. Saisana, S. Tarantola, Global Sensitivity Analysis, John Wiley & Sons Ltd, 2008.
- [27] I. Taha, A. El-Sabbagh, G. Ziegmann, Modelling of strength and stiffness behaviour of natural fibre reinforced polypropylene composites, *Polym. Polym. Compos.* 16 (5) (2008).
- [28] B.D. Agarwal, L.J. Broutman, K. Chandrashekhara, Analysis and performance of fiber composites, John Wiley & Sons, 2006.
- [29] L. Brunacker, Short Carbon Fiber-Reinforced Thermoplastic Composites for Jet Engine Components (Degree project), Luleå University of Technology, 2008.
- [30] Mitsubishi Rayon Co., PYROFIL MR 70 12P, 2014.
- [31] I.M. Daniel, O. Ishai, Engineering Mechanics of Composite Materials, Oxford University Press, 2006.
- [32] M. Alves, Y. Li, S. Pimenta, Spatial variability and characteristic length-scales of strain fields in tow-based discontinuous composites: Characterisation and modelling, *Compos. B Eng.* 262 (2023) 110789.
- [33] P. Feraboli, T. Cleveland, P. Stickler, J. Halpin, Stochastic laminate analogy for simulating the variability in modulus of discontinuous composite materials, *Compos. A Appl. Sci.* 41 (2010) 557–570.
- [34] A.J. Sadowski, J. Michael Rotterand, T. Reinke, T. Ummenhofer, Statistical analysis of the material properties of selected structural carbon steels, *Struct. Saf.* 53 (2015) 26–35.
- [35] M.S. Kim, W.I. Lee, W.S. Han, A. Vautrin, Optimisation of location and dimension of SMC precharge in compression moulding process, *Comput. Struct.* 89 (2011) 1523–1534.
- [36] S.G. Kravchenko, D.E. Sommer, B.R. Denos, W.B. Avery, R. Byron Pipes, Structure-property relationship for a prepreg platelet molded composite with engineered meso-morphology, *Compos. Struct.* 210 (2019) 430–445.